Commun. Math. Phys. 141, 619–631 (1991)

Communications in
Mathematical
Physics

Equilibrium Statistics of a Vortex Filament with Applications

Alexandre Joel Chorin*

Department of Mathematics, University of California, Berkeley, CA 94720, USA

Received March 25, 1991

Abstract. The thermodynamic functions and scaling exponents (including the Kolmogorov and Flory exponents) of a vortex filament in thermal equilibrium are calculated, giving a quantitative content to earlier qualitative analyses. The numerical results uncover a percolation property of vortex filaments near the maximum entropy state. The implications of the results for the onset of turbulence, for the structure of its inertial range, and for superfluid vortices are discussed. In particular, it is shown that vortex stretching pushes a vortex system to a polymeric state and a Kolmogorov spectrum.

Introduction

In an earlier paper [9] it was suggested that some properties of turbulent flow as well as of superfluid flow can be studied through the analysis of the statistical equilibria of vortex filaments. In particular, it was suggested that the inertial range of scales is in approximate thermal equilibrium, and it was shown that the vortex equilibrium of maximum entropy has a Kolmogorov spectrum. Other properties of turbulent vortices, in particular vortex folding, were also explained by an equilibrium model, and an analogy with an ansatz recently proposed in an XY model and in superfluidity was pointed out.

The goal of the present paper is to flesh out these ideas with a quantitative analysis of vortex equilibria. In particular, the energy and the entropy will be calculated as a function of the temperature and the vortex length, and the scaling exponents, in particular the Flory and Kolmogorov exponents for a filament, will be tabulated. A single filament will be considered, for reasons explained below. The calculations reveal an interesting percolation property of vortex filaments near the maximum entropy state that consists of "polymeric" configurations and has a

* This work was supported in part by the Applied Mathematical Sciences subprogram of the Office of Energy Research, U.S. Department of Energy, under contract DE-AC03-76SF-00098, and in part by the National Science Foundation under grant number DMS89-19074

Kolmogorov spectrum. This percolation property provides an explanation of the mechanics that create the maximum entropy state; in brief, the maximum entropy state lies at the boundary between positive and negative temperature states; a vortex of negative temperature is driven towards that boundary by vortex stretching, and a vortex of positive temperature is driven towards that boundary by an energy cascade.

A Review of the Properties of Vortex Filaments

Consider a "vortex" filament that consists of N oriented links that coincide with the edges of a regular cubic lattice of mesh h in three space dimensions. Do not require the filament to be closed (see the discussion below). Ensure that the filament is self-avoiding, i.e., that no point is the end point of more than two links, and thus in particular, no two links coincide. Let i be a multi-index that denotes the location of a link, and let $\underline{\xi}_i$ be the corresponding "vorticity" vector. For simplicity, assume the filament has "circulation" 1, and thus $\underline{\xi}_i$ is a vector of length h pointing in one of six directions. (This construction is carried out in detail in [3, 6].) Assume that the energy of the filament is given by

$$E=\frac{1}{8\pi}\sum_i \sum_{j\neq i} \frac{\underline{\xi}_i \cdot \underline{\xi}_j}{|i-j|}, \tag{1}$$

where $|i-j|$ is the distance between i and j. The expression (1) is a plausible lattice cartoon of the energy of a vortex system [15]:

$$\text{Energy}=\frac{1}{8\pi}\int d\underline{x}\int d\underline{x}' \frac{\underline{\xi}(\underline{x})\cdot\underline{\xi}(\underline{x}')}{|\underline{x}-\underline{x}'|},$$

where $\underline{\xi}$ is the vorticity field and $\underline{x}$ is the spatial variable.

In Eq. (1) we neglect the "self-energy" of the segment, i.e., the contribution to that portion of the six-dimensional $(\underline{x}, \underline{x}')$ space where $\underline{x}$ and $\underline{x}'$ belong to the same link. As discussed in [3, 4, 6], the self-energy is negligible for a vortex of finite length, or having a smooth core, or one that is sufficiently smooth in the direction of its axis. We shall assume that one of these conditions is satisfied.

Assume that the probability of obtaining a given vortex configuration is proportional to the Gibbs weight $\exp(-E/T)$, where E is the energy (1) and T is a temperature. Both positive and negative values of T must be allowed [9], as in the statistical mechanics of vortices in the plane [21]; remember that a negative temperature is "hotter" than a positive temperature [16]. Consider a vortex filament of N links, and define the quantity

$$\mu_{1,N}=\frac{\log\langle r_N\rangle}{\log N},$$

where r_N is the end-to-end length of the vortex, and $\langle\ \rangle$ denotes an average with respect to the Gibbs weight. Let μ_1 be the limit of $\mu_{1,N}$ as $N\to\infty$. If $T=\pm\infty$, all configurations of equal length are equally probable; self-avoiding configurations of equal weight are a standard model of polymer statistics [11], and we shall consistently call the case $T=\pm\infty$ the polymeric case. In the polymeric case μ_1 is the Flory exponent, $\mu_1\cong 0.59$ [18]. We shall call $\mu_{1,N}$ the "Flory exponent" even if $T\neq\infty$ and even in the cases where the limit $N\to\infty$ has not yet been reached.

For large N, $r \equiv \langle r_N \rangle \sim N^{\mu_1}$, and thus $N \sim r^{1/\mu_1}$. It follows that $D_1 = 1/\mu_1$ is the fractal dimension of the filament. If the filament has a non-trivial cross-section and ξ has a support of dimension D_0, then $D_0 - D_1$ is the fractal dimension of a generalized cross-section of the filament.

Define the function

$$\phi(r) = \sum_{|i-j| \leq r} \xi_i \cdot \xi_j ,$$

and let

$$\mu_{2,N} = \frac{\log \langle r_N \rangle}{\log \langle \phi(\langle r_N \rangle) \rangle} . \tag{2}$$

$\phi(r)$ is the integral of the two point correlation function of ξ over a sphere of radius r; its derivative divided by the area of the surface of the sphere is the two point correlation function, and a Fourier transform then yields an energy spectrum for the resulting velocity field of the form $E(k) \sim k^{-1/\mu_2}$ for large k, where $\mu_2 = \lim \mu_{2,N}$ as $N \to \infty$. If the support of the vorticity has dimension D_0, a simple accounting for the cross-section yields $E(k) \sim k^{-\gamma}$, where γ, the generalized Kolmogorov exponent, is $\gamma = D_0 - D_1 + D_2$, $D_2 \equiv 1/\mu_2$ (see [9]). We shall refer to the expression $D_0 - D_{1,N} + D_{2,N}$, where $D_{1,N} = 1/\mu_{1,N}$, $D_{2,N} = 1/\mu_{2,N}$, as the Kolmogorov exponent even when N is finite. We shall assume that the simplified expression

$$\mu'_{2,N} = \frac{\log \langle r_N \rangle}{\log \langle \phi(r_N) \rangle}$$

satisfies $\mu'_{2,N} \sim \mu_{2,N}$; μ' is easier to calculate. $\mu_{1,N}$, $\mu_{2,N}$ satisfy the following inequalities:

$$0 \leqq \mu_{1,N} \leqq 1 ,$$

$$1 \leqq \mu_{2,N} < \infty ,$$

which follow from their definitions.

At equilibrium, it is plausible to assume that $D_0 = 3$ [8]; the results below and in [9] show that at $T = \pm\infty$, $D_0 - D_1 + D_2 \sim 1.68$, close enough to the Kolmogorov value $\gamma = 5/3$ for us to assert that at $T = \infty$ the energy spectrum has the Kolmogorov form. The relation $T^{-1} = \partial S / \partial E$, where S is the entropy and $E = \langle E \rangle$, shows that at $T = \infty$ S has a maximum. Thus the equilibrium of maximum entropy has a Kolmogorov spectrum. We shall also show below that $T = \pm\infty$ is the lowest accessible temperature (it is a low temperature because it is lower than all negative temperatures), and that vortex stretching lowers temperature. Thus vortex stretching drives a vortex to its lowest temperature and largest entropy state. A more detailed discussion of the dynamics will be given below.

Numerical Algorithms and Computational Errors

To generate self-avoiding walks (SAWs) with the Gibbs weight $\exp(-E/T)$, we couple a Monte-Carlo pivot algorithm [14, 18] with Metropolis rejection. In the pivot algorithm one constructs a sequence of equal probability SAWs (=polymers) by repeatedly trying to fold the previous member in the sequence and accepting the outcome if it is self-avoiding. The algorithm requires $O(N)$

operations to produce a new polymer independent of earlier ones. To impose the weighting, one calculates the energy E_{new} of a proposed self-avoiding configuration, and, remembering the energy E_{old} of the previous configuration, one accepts the new one with probability $p=\min[1, \exp((E_{old}-E_{new})/T)]$. The calculation of the energy requires $O(N^2)$ operations, as the fast summation algorithms that have become available are ineffective with relatively small values of r and N, and thus the calculations with T finite must be much less extensive than what can be done with $T=\infty$. Fortunately, it will turn out that only qualitative information is really needed at T finite. For further details, see [9, 18].

To start a Monte-Carlo run one needs an initial state. We shall start with a straight line of N links (which is certainly self-avoiding) and before beginning to calculate averages, perform N Monte-Carlo steps just to begin the process of forgetting the initial conditions.

The dependence of the results on N, the number of links in the filament, and on T will be discussed in detail below. We wish now to discuss briefly the dependence of the results on n, the number of Monte-Carlo steps. With n too small, the phase space is inadequately covered and statistical error appears. We shall be making numerous runs with various values of T and N and can afford to make a few longer runs to assess the error. One expects the error to grow as $|T|$ decreases (because the probability p can then be small and new configurations are generated at a lower rate), and with N (critical slowing down, e.g. [18]). These expectations are fulfilled.

One way to measure the error is to compare the results of a very long run with the results of a run of standard length. Another way is to make a number of independent runs and calculate the standard deviation of the results (which should scale with $n^{-1/2}$). The two methods give consistent answers. We need most accuracy at $T=\infty$ and shall use $n=3\times 10^6$ at that value of T. The errors in the mean energy, the entropy, μ_1 and μ_2 are then around 1% for $50\leqq N\leqq 350$. At $T=+1$, with $n=3\times 10^5$, the errors vary between 2 and 3 percent, and at $T=-1$, with $n=3\times 10^5$, they vary between 2% at $N=100$ and 10% at $N=350$. For values of $|T|$ between 0.4 and 1, and $n=3\times 10^5$ or $n=3\times 10^6$, the results are unreliable but suggestive, and for $|T|<0.4$ they are completely unreliable. The errors in μ_2 grow fastest as $|T|$ decreases and μ_2 will not be displayed when they are too large.

We shall be evaluating the entropy by a variant of an algorithm due to Meirovitch [19]. Consider m neighboring links on the filament, and their relative configurations $C_1, C_2, \ldots, C_q$. Estimate S/N, the entropy per link, by

$$\frac{S}{N}=-\frac{1}{m}\sum_i P(C_i)\log P(C_i),$$

where $P(C_i)$ is the probability of the i^{th} configuration estimated as the frequency of its occurrence in a Monte-Carlo run. We shall usually use $m=3$ and $q=150$ (=the number of SAWs of 3 links). An increase in m and q has no perceptible effect on the results. The algorithm has been validated in the case of a random walk with independent increments (where $S/N=\log 6$) and its analogue has been thoroughly tested in a two-dimensional Ising model.

It is the availability of the pivot algorithm and its modification that makes us adhere to the study of an unclosed filament. There does not seem to be an algorithm of similar efficiency that can be used to study a closed loop. Open filaments are natural in one of the applications below, and must be explained away in the two others. The explanation is that an open filament can be closed by a few bendings which should not affect the thermodynamic functions unduly. No quantitative assessment of this explanation is available.

The Thermodynamic Functions

We begin by plotting the calculated mean energy $\langle E \rangle$ and mean entropy $\langle S_N \rangle$ of a single filament of N links as a function of T and N. For simplicity, we pick a mesh spacing on the lattice $h=1$. We shall write for short E for $\langle E_N \rangle$ and S for $\langle S_N \rangle$.

In Fig. 1 we display the variation of E as a function of $\beta=1/T$ for $-2.5 \leqq \beta \leqq 2.5$. Note that as β varies from 2.5 to 0 and then to -2.5, T varies from 0.4 to infinity, and then from infinity to -0.4 (the sign of infinity is immaterial); thus T is monotonically increasing. Note that E is increasing with T for all values of N. In Fig. 2 we display the variation of E with N for fixed values of T. Note that the

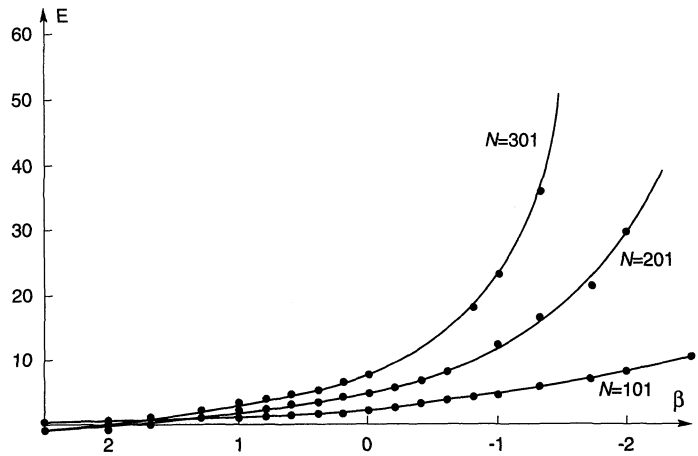

Fig. 1. Energy as a function of $\beta=T^{-1}$

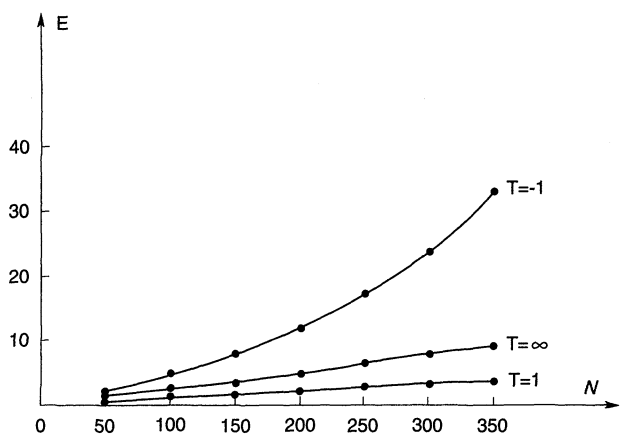

Fig. 2. Energy as a function of N

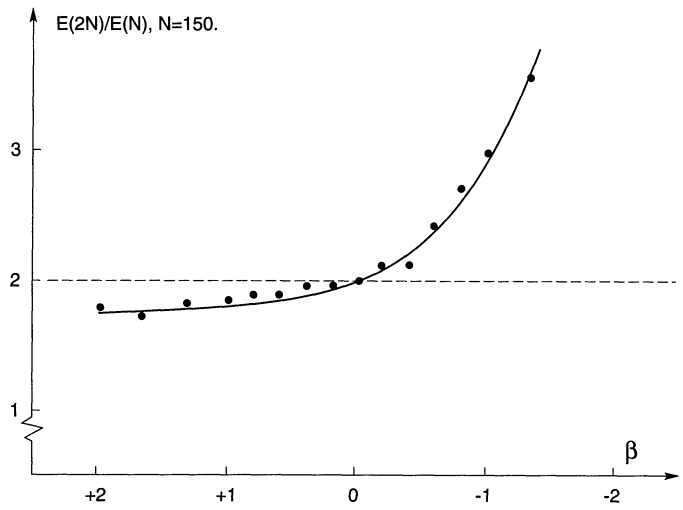

Fig. 3. $E(2N)/E(N)$ as a function of β

increase of E with N is sublinear for $T>0$ and superlinear for $T<0$. To hammer home this important point we display in Fig. 3 the ratio $E(2N)/E(N)$ as a function of β for $N=150$. When that ratio is less than 2 the growth of E is sublinear and when the ratio is larger than 2 the growth is superlinear. The data points are not error-free (see the preceding section) and the solid curve is drawn in a way that seems plausible to the naked eye. The fact that for $T=\infty$, $E(2N)/E(N)=2$ is one of the scaling properties of the energy (1) discussed in [4].

Consider the dependence of the curves in Fig. 1 on h. Suppose h is halved and N doubled, so that Nh is constant. E in (1) is a linear function of h (because $|\xi_i|$, $|\xi_i|$, and $|i-j|$ are each linear functions of h). If N is doubled, E grows by more than 2 for $T<0$ and by less than 2 for $T>0$, thus the net effect of doubling N and halving h is to decrease E for $T>0$ and increase E for $T<0$. The curves in Fig. 1 grow more steeply for $T<0$ and are flatter for $T>0$. The curve for $T=\pm\infty$ is invariant.

In Fig. 4 we display the variation of the entropy per link S/N as a function of β for $N=351$. Note that S has a maximum at $T=\infty$ ($\beta=0$), as expected. The slope of S is much smaller on the positive T side than on the negative T side, as can be expected from the larger values of E for $T<0$ and from the relation $T^{-1}=\partial S/\partial E$. Further, note that S/N varies little with N in the range where the calculation can be trusted, and thus S increases with N. The larger the filament, the larger its entropy. In the case $T=\infty$ the filament is a polymer, and in that context this result is well known [11]. The connection of this observation with known facts about vortex stretching is discussed below in the section on the onset of turbulence.

A single filament calculation should be a faithful representation of the behavior of a member of a sufficiently dilute suspension of such filaments. The dependence of E and S on the number of links in several nearby, strongly interacting filaments should be roughly the same as the dependence on N exhibited here. Since in the classical (i.e. non-quantum) vortex case there is no relation between T and filament density, one can pick arbitrarily the division of N links between a number of neighboring filaments, and the choice we made here of considering a single one is easy and reasonable. The relation of the resulting independent filament model to the independent loop approximation is superfluidity is discussed in [9].

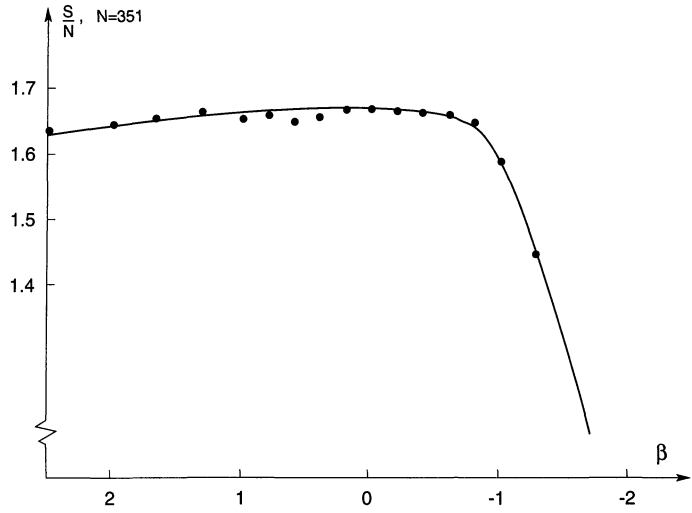

Fig. 4. Entropy per link as a function of β

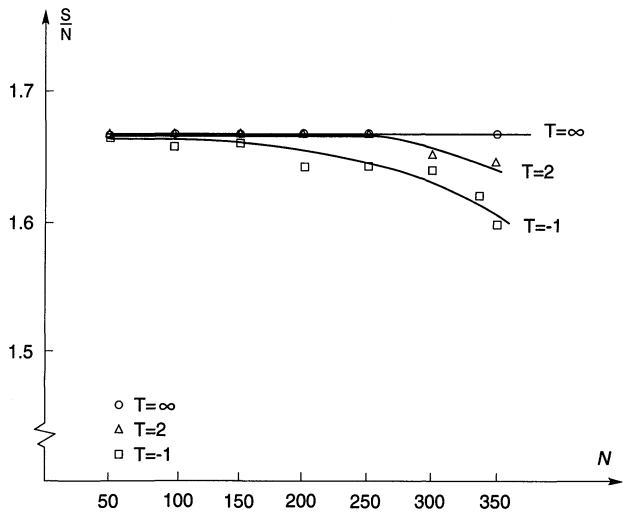

Fig. 5. Entropy per link as a function of N

The Scaling Laws and Vortex Percolation

In Figs. 6 and 7 we display the variation of $\mu_{1,N}$ and $\mu_{2,N}$ with N for various values of β. Observe first that

$$\lim_{N\to\infty} \mu_{1,N} = \begin{cases} 1, & T<0, \\ \mu_1, & T=\infty, \\ 0, & T>0, \end{cases}$$

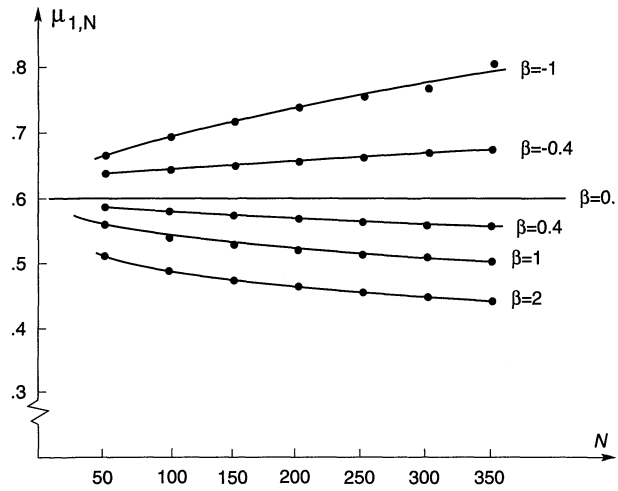

Fig. 6. The Flory exponent as a function of N

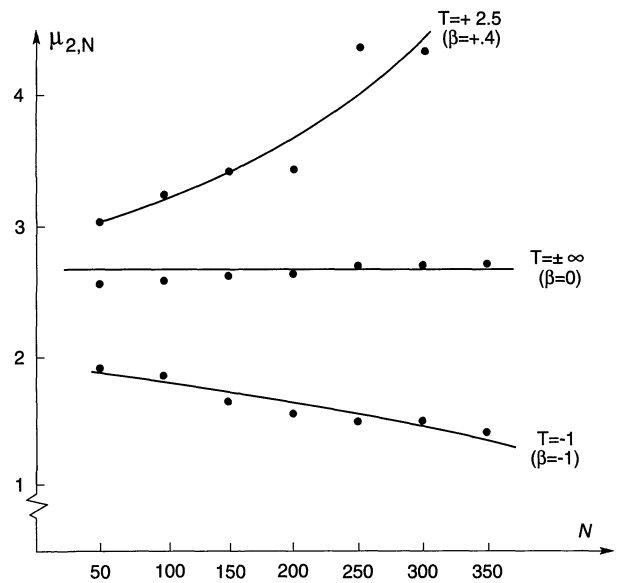

Fig. 7. The correlation exponent $\mu_{2,N}$ as a function of N

and

$$\lim_{N\to\infty} \mu_{2,N} = \begin{cases} 1, & T<0, \\ \mu_2, & T=\infty, \\ \infty, & T>0, \end{cases}$$

where μ_1 is the Flory exponent $\mu_1 = 0.592 \pm 0.005$ and $\mu_2 = 2.70 \pm 0.05$. The limiting values for T finite are the maximum and minimum values that $\mu_{1,N}, \mu_{2,N}$

can take, and are reached if the trends in Figs. 6 and 7 continue. The corresponding limiting values of γ are:

$$\lim_{N\to\infty}\gamma_N=\begin{cases}3, & T<0,\\ \gamma_0, & T=\infty,\\ \infty, & T>0,\end{cases}$$

where $\gamma_0=1.68\pm0.01$.

Before discussing the meaning of these limits, note that if one remains within a range of wave numbers k such that $L^{-1}<k<h^{-1}$, where L is a length typical of the overall extent of the vortex filament, the scaling analysis in the review section above holds and yields a spectrum of the form $E(k)\sim k^{-\gamma_N}$, where γ_N is a function of N (or equivalently, of the total energy). On these scales, the spectrum appears to be multifractal [24]. It is clear that for any N, if $T<0$ then $\gamma_N>\gamma_0$, and if $T>0$, $\gamma_N<\gamma_0$.

The meaning of the limiting values μ_1, μ_2, γ is quite clear: If a vortex at negative temperature has a high energy (or is very long) it becomes smooth ($\mu_1=1$) and its spectrum corresponds to the spectrum of a smooth flow $\gamma\geqq3$ [5]. The value $\gamma=3$ is picked out because our calculation of the spectrum was based on a filament model; more general smooth vortices may have larger γ's. The meaning of the limits for $T>0$ is less transparent. Consider μ_1. If $\mu_1=0$, $r\sim N^0$, i.e., the end-to-end length of the vortex does not increase with N, and the vortex rolls up into a tight "ball." This means that the vortex will not span large distances. The temperature $T=\infty$ ($\beta=0$) is thus a percolation threshold: infinitely extended vortices can exist on one side but not on the other. The threshold corresponds to a maximum entropy and to polymeric configurations (for a relevant introduction to percolation, see [12]).

Consider again what happens if N is increased while the length of the vortex Nh remains fixed. E in (1) is a linear function of h. If h is halved and N is doubled, E more than doubles for $T<0$ and grows by less than a factor of 2 for $T>0$ (Fig. 3). Thus E increases for $T<0$ and $\mu_{1,N}, \gamma_N$ move further from the polymeric values μ_1, γ_0, while for $T<0$ $\mu_{1,N}$ and γ_N approach μ_1 and γ_0.

Note that $T=\infty$ is the maximum entropy state, as is usual, but it is a low temperature state. $T=\infty$ is the lowest temperature accessible to a long filament. Furthermore, γ_0 is the only exponent less than 3 for which $E(k)\sim k^{-\gamma}$ holds as $k\to\infty$ independently of lattice spacing.

Application to the Onset of Turbulence

Consider a flow with a few well defined vortices that is nearly stationary (for example, a thin vortex ring propagating at a constant velocity to which a small perturbation has been recently applied). Initially, the rate of growth of line length is not large, and the vortices can be viewed as having an approximately constant length. The time evolution of the vortex system is then approximately scanning the possible states of a constant length vortex filament system, and averages can be calculated as if the system were at equilibrium. That equilibrium is slowly drifting because of the change in vortex length.

The initial temperature T of the system is negative, with $|T|$ small, since the vortex lines are smooth. The increase in vortex length corresponds to an increase in

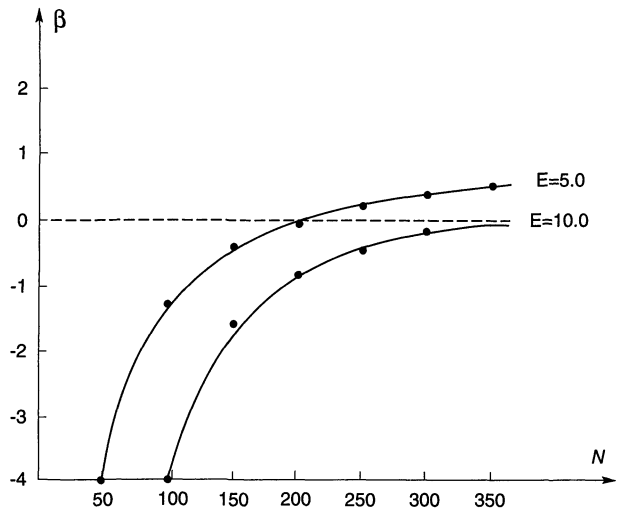

Fig. 8. The temperature as a function of N at constant energy

entropy (see above). This observation is in agreement with the conclusions in earlier work [7, 8] that vortex line length or integral quantities that measure it can be used as entropies for a vortex system. An interesting converse is provided by Cocke's result [10], which can be interpreted as stating that line length in isotropic homogeneous incompressible flow increases when the entropy increases [7].

Since $\langle E \rangle$ is an increasing function of both T and N, an increase in N requires a decrease in T. In Fig. 8 we plot the values of $\beta = T^{-1}$ needed to keep $\langle E \rangle$ constant as N is increased for two values of $\langle E \rangle$. These values are obtained by considering what happens along a horizontal line in Fig. 1. Note that as $h \to 0$, the curves to the right of the curve $\beta = 0$ become flatter, and thus a large change in N corresponds, for $T > 0$, to a small change in μ_1 and γ. The curve for $\beta = 0$ is thus an approximate barrier, the more so as N increases or h decreases. This fact is reflected in Fig. 8. Note that the asymptote is not $T = 0$ but a finite value that approaches $T = \infty$ ($\beta = 0$) as $\langle E \rangle$ or N is increased. If N is increased while h is decreased the polymeric boundary is reached sooner, as can also be deduced from the earlier discussion of the limit $h \to 0$. An increase in N corresponds to vortex stretching (with an attendant energy cascade), while a decrease in h with $Nh = \text{constant}$ describes an energy cascade to small scales without overall stretching; thus vortex stretching causes the temperature to decrease to $T = \pm\infty$, while the energy cascade prevents further folding and further decrease in μ_1 and γ. In the present discussion, only the left part of the figure can correspond to a flow that satisfies our assumption of near equilibrium; in a time dependent calculation the rate of change of N typically increases and thus the rest of the curve has a suggestive but maybe not a deductive value.

As T decreases, $\mu_{1,N}$ decreases and thus the Hausdorff dimension D_1, which measures the folding of the vortex on scales larger than h, increases. In Fig. 9 we plot the values of $\mu_{1,N}$ as a function of N for two values of $\langle E \rangle$. $\mu_{1,N}$ decreases and the vortex must fold. For heuristic discussions of this phenomenon, see [3, 4, 7]. In a time dependent flow, the increase in D_1 manifests itself in the formation of small-scale "hairpins" or loops, as documented also in the solutions of the Euler or Navier-Stokes equations, see e.g. [1, 2, 17].

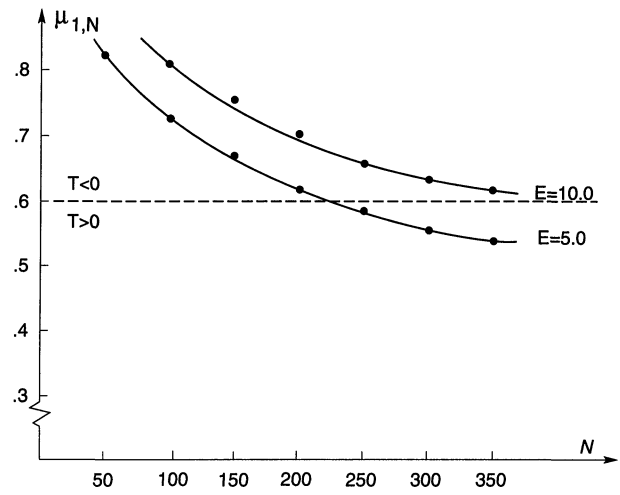

Fig. 9. $\mu_{1,N}$ as a function of N at constant energy

The decrease of T from $\pm\infty$ to 0 has no further effect on the formation of loops, folding, μ_1 and γ if the lattice spacing h size has been allowed to tend to zero. For finite h, $T=\pm\infty$ ($\beta=0$) is an approximate asymptote for the temperature at large enough N or E. The boundary $\mu_1=0.59$ can be crossed in particular if the range of allowed scales is truncated, e.g. by viscosity or by discretization in a numerical scheme. Once that boundary is crossed, the loss of percolation forces the vortex strands to reconnect into smaller loops (as, for example, in the Crow instability). Maximum entropy occurs at infinite temperature, as one expects; what is unexpected is that this infinite temperature is a low temperature.

Note further that $\partial E/\partial N$ decreases as T decreases, in agreement with the observation that vortex stretching facilitates further stretching (see for example the discussion of this fact in [2]).

The Inertial Range

We can once again apply the assumption of near equilibrium once fully developed turbulence has been established. According to the model developed in [9], the inertial range of scales can be viewed as a thermal equilibrium at small scales perturbed through the addition of energy at its large scale end and the removal of energy at the small scale end. The calculation in [9] shows that the perturbation is not large.

Consider first the small scale (large wave number k) equilibrium. Its temperature must be $T=\pm\infty$ (and thus $\gamma=\gamma_0$) for several reasons:

(1) γ_0 is the only non-trivial exponent γ such that $E=k^{-\gamma}$ is a possible approximation to the spectrum for all k large enough.
(2) Vortex stretching pushes the vortex system towards $T=\infty$ and $\gamma\sim 1.68$; the persistence of an initial range to $k\to\infty$ and the impossibility of having very long vortices below the percolation threshold forbids a crossing to $T>0$ and smaller γ.

Note that macroscopic vortices appear infinitely long on inertial scales.
(3) It is plausible that what is actually observed at equilibrium is a maximum probability (and thus a maximum entropy) state. Note that in two-dimensional flow maximum entropy states describe well what is actually observed [22].

The perturbation of this equilibrium by a small viscosity was described in [9]. The addition of viscosity cuts off the large k part of the spectrum and makes possible some transitions to the positive T range. Numerical experiments with time dependent flow, to be presented elsewhere, show that the convoluted vortex lines near $\mu_1 \sim 0.6$ respond by reconnecting and changing topology. An energy cascade and vortex reconnection are thus closely connected. Note that the picture of the inertial range that is offered here differs radically from earlier ones.

This picture does agree with the observation in [20] that in many fluid systems the maximum entropy and the minimum dissipation states coincide.

Superfluid ^{4}He and the λ-Point

The λ-transition from a superfluid to a normal state in ^{4}He in three space dimensions has been characterized by the growth of small vortex loops into macroscopic vortex loops [23, 25, 26], in analogy with the Kosterlitz-Thouless mechanism familiar from two space dimensions [13]. Shenoy [23] analyzed the transition by a Kosterlitz-Thouless renormalization scheme into which he introduced an ansatz that can be interpreted as assuming that at the transition $\mu_1 \sim 0.6$, our value at $T = \infty$.

It is attractive to consider the λ-transition as a percolation threshold. For $T < T_\lambda$ the vortices are small, for $T \geqq T_\lambda$ they can acquire an infinite radius. At the percolation threshold, we have seen that $\mu_1 \sim 0.6$.

However, there are differences. At the λ-point, T is small ($T = k \cdot T_\lambda^0 = 1.38 \cdot 10^{-16} \times 2.18$ ergs, where k = Botzmann's constant). To claim that this temperature is relatively large one would need an estimate of h, which we have not identified. In the superfluid case, the interactions between the vortices and other excitations are large enough to keep the temperature positive and constant. Vortex loops can appear as a result of thermal fluctuations, and a given loop polarizes the medium and decreases the interaction energy. We do not yet know how to account for all these effects and unambiguously relate the Shenoy ansatz to the previous discussion.

Conclusions

We believe that the discussion in this paper provides a convincing testimony to the usefulness of vortex statistics in the study of turbulence and of quantum fluids, and in particular, makes plausible the near-equilibrium theory of the inertial range.

There are other applications for this analysis. One direction that we are pursuing is the thermodynamical analysis of numerical methods, in particular vortex methods, so as to ensure their long-time convergence in a turbulent regime.

Acknowledgements. I would like to thank Professor G. Williams for a helpful letter, and Mr. T. Ligocki for help with running the calculations.

References

1. Bell, J., Marcus, D.: The evolution of a perturbed vortex filament, Report UCRL-JC-105029, Lawrence Livermore Laboratory, 1990
2. Chorin, A.J.: The evolution of a turbulent vortex. Commun. Math. Phys. **83**, 517–535 (1982)
3. Chorin, A.J.: Turbulence and vortex stretching on a lattice. Commun. Pure Appl. Math. **39** (special issue), S47–S65 (1986)
4. Chorin, A.J.: Scaling laws in the lattice vortex model of turbulence. Commun. Math. Phys. **114**, 167–176 (1988)
5. Chorin, A.J.: Spectrum, dimension and polymer analogies in fluid turbulence. Phys. Rev. Lett. **60**, 1947–1949 (1988)
6. Chorin, A.J.: Constrained random walks and vortex filaments in turbulence theory. Commun. Math. Phys. **132**, 519–536 (1990)
7. Chorin, A.J.: Vortices, turbulence and statistical mechanics. In: Vortex flows and vortex methods. Gustafson, K., Sethian, J. (eds.). SIAM, 1991
8. Chorin, A.J.: Statistical mechanics and vortex motion, to appear in the Proc. 1990 AMS/SIAM Summer School. Anderson, C., Greengard, C. (eds.)
9. Chorin, A.J., Akao, J.: Vortex equilibria in turbulence theory and quantum analogues. Physica D, in press (1991)
10. Cocke, W.J.: Turbulent hydrodynamic line stretching: consequences of isotropy. Phys. Fluids **12**, 2490–2492 (1969)
11. de Gennes, P.G.: Scaling concepts in polymer physics. Cornell University Press 1971
12. Grimmett, G.: Percolation. Berlin, Heidelberg, New York: Springer 1989
13. Kosterlitz, J., Thouless, D.J.: Order, metastability and phase transitions in two dimensional systems. J. Phys. C: Solid State Phys. **6**, 1101–1203 (1973)
14. Lal, M.: Monte Carlo computer simulations of chain molecules. Molecular Phys. **17**, 57–64 (1969)
15. Lamb, H.: Hydrodynamics. NY: Dover 1932
16. Landau, L., Lifshitz, L.: Statistical physics, 3rd edition, part 1. New York: Pergamon Press 1980
17. Lesieur, M.: Turbulence et structures cohérentes dans les fluides. Nonlinear partial differential equations and their applications. Collège de France seminar 1989–1990. Brezis, H., Lions, J.L. (eds.). Paris: Pitman Press 1990
18. Madras, N., Sokal, A.: The pivot algorithm: a highly efficient Monte Carlo method for self-avoiding walks. J. Stat. Phys. **50**, 107–186 (1988)
19. Meirovitch, H.: A Monte Carlo study of the entropy, the pressure, and the critical behavior of the hard sphere lattice gas. J. Stat. Phys. **30**, 681–698 (1984)
20. Montgomery, D., Phillips, L.: Minimum dissipation and maximum entropy. In: Maximum entropy and Bayesian methods. Fougère, P.F. (ed.). The Netherlands: Kluwer 1990
21. Onsager, L.: Statistical hydrodynamics. Nuovo Cimento. [Suppl.] **6**, 279–287 (1949)
22. Robert, R.: A maximum entropy principle for two dimensional perfect fluid dynamics (to appear) (1991)
23. Shenoy, S.R.: Vortex loop scaling in the three dimensional XY ferromagnet. Phys. Rev. B **40**, 5056–5068 (1987)
24. Sreenivasan, K.R., Meneveau, C.: The fractal aspects of turbulence. J. Fluid Mech. **173**, 357–386 (1986)
25. Williams, G.: Vortex ring model of the superfluid λ transition. Phys. Rev. Lett. **59**, 1926–1927 (1987)
26. Williams, G.: Vortices and the superfluid ^{4}H transition in two and three dimensions. Proc. Exeter Conf. Excitations and Quantum Fluids. Wyatt, A.F.A. (ed.). NATO, 1990

Communicated by A. Jaffe